Asymmetric localizations of the ABC transporter PaPDR1 trace paths of directional strigolactone transport

Sasse, Joëlle ; Simon, Sibu ; Gübeli, Christian ; Liu, Guo-Wei ; Cheng, Xi ; Friml, Jiří ; Bouwmeester, Harro ; Martinoia, Enrico ; Borghi, Lorenzo

Abstract: Strigolactones, first discovered as germination stimulants for parasitic weeds [1], are carotenoid-derived phytohormones that play major roles in inhibiting lateral bud outgrowth and promoting plant-mycorrhizal symbiosis [2-4]. Furthermore, strigolactones are involved in the regulation of lateral and adventitious root development, root cell division [5, 6], secondary growth [7], and leaf senescence [8]. Recently, we discovered the strigolactone transporter Petunia axillaris PLEIOTROPIC DRUG RESISTANCE 1 (PaPDR1), which is required for efficient mycorrhizal colonization and inhibition of lateral bud outgrowth [9]. However, how strigolactones are transported through the plant remained unknown. Here we show that PaPDR1 exhibits a cell-type-specific asymmetric localization in different root tissues. In root tips, PaPDR1 is co-expressed with the strigolactone biosynthetic gene DAD1 (CCD8), and it is localized at the apical membrane of root hypodermal cells, presumably mediating the shootward transport of strigolactone. Above the root tip, in the hypodermal passage cells that form gates for the entry of mycorrhizal fungi, PaPDR1 is present in the outer-lateral membrane, compatible with its postulated function as strigolactone exporter from root to soil. Transport studies are in line with our localization studies since (1) a papdr1 mutant displays impaired transport of strigolactones out of the root tip to the shoot as well as into the rhizosphere and (2) DAD1 expression and PIN1/PIN2 levels change in plants deregulated for PDR1 expression, suggestive of variations in endogenous strigolactone contents. In conclusion, our results indicate that the polar localizations of PaPDR1 mediate directional shootward strigolactone transport as well as localized exudation into the soil.

DOI: https://doi.org/10.1016/j.cub.2015.01.015

Asymmetric localizations of the ABC transporter PaPDR1 trace paths of directional strigolactone transport

*Joëlle Sasse[1], Sibu Simon[2], Christian Gübeli[1], Guo-Wei Liu[1], Xi Cheng[3], Jiří Friml[2], Harro Bouwmeester[3], Enrico Martinoia[1] and Lorenzo Borghi[1]**

[1] Institute of Plant Biology, University of Zürich, 8008 Zürich, Switzerland

[2] Institute of Science and Technology Austria, 3400 Klosterneuburg, Austria

[3] Wageningen UR, Wageningen University, 6708 PB Wageningen, The Netherlands

* Correspondance : lorenzo.borghi@uzh.ch, phone: ++41 (0)44 63 48276, fax.: ++41 (0)44 63 48204

Summary

Strigolactones (SL), firstly discovered as germination stimulants for parasitic weeds [1], are carotenoid-derived phytohormones that play major roles in inhibiting lateral bud outgrowth and promoting plant-mycorrhizal symbiosis [2-4]. Furthermore it was shown that strigolactones are involved in the regulation of lateral and adventitious root development, root cell division [5, 6], secondary stem growth [7] and leaf senescence [8]. Recently, we discovered the strigolactone transporter *Petunia axillaris* PLEIOTROPIC DRUG RESISTANCE 1 (PaPDR1), which is required for efficient mycorrhizal colonization and inhibition of lateral bud outgrowth [9]. However, how strigolactones are transported through the plant remained unknown. Here we show that PaPDR1 exhibits a cell-type, specific asymmetric localization in different root tissues. In root tips, PaPDR1 is co-expressed with the strigolactone biosynthetic gene *DAD1 (CCD8)* and it is localized at the apical membrane of root hypodermal cells, presumably mediating the shootward transport of strigolactone. Above the root tip, in the hypodermal passage cells (HPCs) that form gates for the entry of mycorrhizal fungi, PaPDR1 is present in the outer-lateral membrane, compatible with its

postulated function as strigolactone exporter from root to soil. Transport studies using radiolabeled strigolactone are in line with our localization studies, since a *papdr1* mutant displays impaired transport of strigolactones out of the root tip to the shoot as well as into the rhizosphere. In line with this, *DAD1* expression and PIN1/PIN2 levels change in plants deregulated for PDR1 expression, suggestive of variations in endogenous strigolactone contents. In conclusion, our results indicate that the polar localizations of PaPDR1 mediate directional shootward strigolactone transport as well as localized exudation into the soil.

A role for PaPDR1 in regulation of strigolactone transport

Strigolactone biosynthesis requires the carotenoid cleavage dioxygenase CCD8 (DAD1/MAX4/D10/RMS1), which together with the iron-binding D27 and CCD7 [4, 10, 11] leads to the biosynthesis of the first strigolactone bio-active molecule, carlactone [12, 13]. Localization of strigolactone biosynthesis was mainly studied via grafting experiments and is reported to take place in root tips and close to shoot axils [14, 15]. Wild-type shoots grafted on roots of strigolactone biosynthetic mutants exhibited a wild-type phenotype, indicating that shoot-derived strigolactone is sufficient to support its function above ground. However, shoot strigolactone mutants can be rescued by grafting on wild-type roots, indicating that strigolactones are also transported from the root to the shoot. This observation is supported by strigolactone detection in the xylem of Arabidopsis and tomato, although this has not been reported from other species [16]. These results and the fact that strigolactone is exported from the root to the soil to induce hyphal branching in mycorrhizal fungi indicates that the routes of strigolactone transport are multiple and complex. Here we investigate the possible role of PaPDR1 in shootward transport of strigolactone out of the root tip as well as out of the hypodermal passage cells into the soil. In the root tip, PaPDR1 activity would avoid strigolactone accumulation in the root meristem, which was reported to be sensitive to small alterations in strigolactone concentration [6]. Out of the root tip, PaPDR1 would help the allocation of strigolactone to its targets in- and outside the plant.

In order to elucidate the localization of PaPDR1, the petunia cultivar W115 and Arabidopsis *rna-dependent rna polymerase6* (*rdr6)* (a mutant that allows stabilized ectopic expression of transgenes otherwise prone to silencing [17]), were transformed with the fusion GFP-gPaPDR1 (GFP-PDR1) under the control either of the native (npPDR1) or the p35SCaMV promoter (PDR1-OE) [9]. We chose this petunia cultivar since W138, used to obtain mutant lines via transposon insertion, is recalcitrant to transformation [18] and we did not succeed to insert transgenes in the *pdr1* mutant transferred into the W115 x W138 background. In order to test GFP-PDR1 functionality in petunia we exposed wild-type and PDR1-OE plants to 2.5 to 40 μM concentrations of the synthetic SL analogue GR24 (Chiralix): 5 days after induction, with GR24 concentrations higher than10 μM, W115 had shorter primary root, decreased lateral root density and higher level of leaf chlorosis than PDR1-OE (Figure S1A-G, L), confirming that GFP-PDR1 is active in petunia, as previously shown in Arabidopsis [9]. This trend was confirmed two weeks after induction, although already 10 days after treatment the only significant difference in lateral root density was due to GR24 inhibition of primary root elongation, suggesting that petunia lateral roots are less sensitive to GR24 than primary root tips (Figure S1H-K). Compatible with the reported SL-induced photosynthetic pathway [19], PDR1-OE are darker green than WT (Figure S1L). We then compared SL-induced germination of the broomrape *Phelipance ramosa* with exudates from W115 or PDR1-OE roots: PDR1-OE induced 2-fold higher germination than WT, compatible with enhanced SL exudation due to GFP-PDR1 overexpression (Figure S1M). Finally we assessed shoot lateral branching in adult plants, a known target of strigolactone transport [9]: the development of lateral branches was inhibited in petunia PDR1-OE plants compared to WT, indicating the presence of ectopic strigolactone transport towards shoot axillary buds (Figure S1N-V). In both petunia and Arabidopsis, GFP-PDR1 levels were low when driven by the endogenous petunia PDR1 promoter (np-PDR1) compared with the PDR1-OE lines (Figure 1A-E), with the strongest signal occurring in the *rdr6* background, where silencing of ectopic transgenes is inhibited [17]. These different GFP-PDR1 amounts fit the limited and rather low expression level observed in *pPDR1:GUS* plants [9]. *PaPDR1* was shown to be induced by

auxin, strigolactone and low phosphate [9]. To boost expression of PaPDR1, we performed our experiments under low nutrient conditions (see Experimental procedures), which are often experienced by plants in natural ecosystems and are known to stimulate mycorrhizal colonization [20]. This allowed us to detect np-PDR1 (Figure 1F, H, I) in petunia root tips one month and two months after germination, respectively, in 20% (n=30) and 60% (n=30) of the analyzed cases. GFP-PDR1 displayed polar localization in the apical/basal domain of hypodermal cells in petunia root tips. The same pattern was visible in the root tips of 2-week-old PDR1-OE plants without starvation treatment in 10% of the analyzed plants (n=50) (Figure 1G).

Previous studies showed that the auxin transporters AtPIN1 and AtPIN2 are basally localized in the root stele and apically in epidermis and cortex cells outside the meristem region [21]. To identify the polarity of the asymmetric PaPDR1 signal, we compared GFP-PDR1 localization with the localization of the *Petunia hybrida* homologues PhPIN1 and PhPIN2. Petunia has a strong auto-fluorescent background in most tissues, although lower in the root tip, therefore immuno-localization was chosen to increase the GFP-to-autofluorescence signal ratio. Immuno-localization with anti- AtPIN1, AtPIN2 or GFP in 2-month-old np-PDR1 plants starved on clay substrate did not show any signal (data not shown). Similarly, GFP-PDR1 immuno-localization in *np-PDR1 Arabidopsis thaliana* were negative (data not shown). Protein co-localizations were then carried out with GFP and AtPIN2 antibodies in 2-week-old PDR1-OE and 4-week-old np-PDR1 petunia plantlets, the latter starved for 2 weeks. GFP-PDR1 in PDR1-OE plants was present and asymmetrically localized in hypodermis and partially overlapping with the PhPIN2 expression domain (Figure 1J-O, Figure 2A-I and Figure S2T). PhPIN2 was present also in cortex layers below the hypodermis in contrast to GFP-PDR1, which was confined to the hypodermis. The hypodermal cells co-expressing both GFP-PDR1 and PhPIN2 (Figure S2T) showed subcellular co-localization of GFP-PDR1 and PhPIN2 in PDR1-OE (Figure 2G-I) and in np-PDR1 roots (Figure 2J-M), indicating that PaPDR1 is targeted to the apical domain of the plasma membrane. As shown by the signal quantification of (Figure 2Z, Z'), the cytosolic PDR1/PIN2 ratio in npPDR1 seedlings is close

to 1, compatible with equal amounts of PDR1 and PhPIN2. PhPIN2 signal exceeds that of PDR1 in the plasma membrane. In PDR1-OE seedlings, the PDR1/PIN2 cytosolic and plasma membrane ratios are higher than 1, as a result of PDR1 ectopic expression driven by p35S. Seedling incubation in 10 μM GR24, previously shown to induce a 4-fold-induction of *PDR1* in 24-hours [9], already after 6-hours increased the localization of PDR1 to the plasma membrane as well as the number of cells co-expressing PDR1 and PhPIN2 (Figure S2T).

Localization of PaPDR1 is shaped by SL and auxin

PIN1 protein was shown to decrease in stems and root tips after application of GR24 [6, 22]. On the other hand, GR24 induced PIN2 apical and vacuolar localization [23]. Also in PDR1-OE root tips PhPIN1 was down- and PhPIN2 up-regulated (Figure S2A-F), compatible with ectopic transport of endogenous strigolactone as also suggested by PDR1-OE shoot phenotype (Figure S1G, L-T). We previously showed that NAA induces pPDR1 [9]. Therefore we tested whether *pPDR1* activity is low in the PIN1 domain, where SL would decrease the auxin induction on *pPDR1*. Indeed, the root-tip expression patterns of the promoter fusions *pPDR1:nls-YFP* and *pPIN1:nls-RFP* showed that *pPDR1* activity is high in epidermis and cortex, where PIN2 is expressed, but excluded from the root stele, where *pPIN1:nls-RFP* signal is present (Figure S2G-L). These results support the hypothesis that strigolactone shapes the pattern of its transporter not only by direct induction of *PaPDR1* expression but also via auxin signaling by differential regulation of PIN1 and PIN2 (Figure S2V).

PaPDR1 is asymmetrically localized in Arabidopsis root tip cells

To explore whether PaPDR1 is also asymmetrically localized in Arabidopsis, for which a functional strigolactone transporter has not yet been identified, we expressed GFP-PDR1 in *Arabidopsis thaliana* [9]. No GFP signal could be detected in Arabidopsis plants expressing the *np-PDR1*, even in the *rdr6* background [17]. Whether this is due to the low protein levels (Figure 1D) or to the petunia promoter not being functional in Arabidopsis is yet to be determined. In contrast GFP-PDR1 was detectable in PDR1-OE Arabidopsis plants (At-

PDR1-OE) in root epidermal, cortex cells and stele (Figure S3A-H). GFP-PDR1 was AtPIN2-like localized (apical) in epidermal and cortex cells, and AtPIN1-like localized (basal) in root stele cells (Figure 2N-S). We assessed that 46% of the analyzed cells in the stele co-express PDR1 and AtPIN1 and 57% of the analyzed hypodermal cells co-express PDR1 and AtPIN2 (Figure S2U). In these cells, GFP-PDR1 co-localizes with AtPIN1 in the stele and GFP-PDR1 co-localizes with AtPIN2 in the epidermis/cortex (Figure S4R-V). GFP-PDR1 localization in epidermal and cortex cells was confirmed to be predominantly asymmetric by co-staining of plasma membranes with FM4-64 (Figure S3I-N).

A similar GFP-PDR1 expression pattern present in both PIN1 and PIN2 domains was also observed in petunia PDR1-OE roots but only after a 6-hour-long incubation with 10 μM GR24. Like in Arabidopsis, also in petunia GFP-PDR1 was then apically localized in the hypodermis and basally in the root stele (Figure 2T-Y and Figure S2T). Protein quantification confirmed that 6-hour-long incubations with 10 μM GR24 increases or stabilizes GFP-PDR1 protein levels (Figure S2O-S). Surprisingly this is a long lasting effect, as increased protein levels could be still detected even 3 weeks after germination on GR24 (Figure S2R-S).

GFP-PDR1 is localized at the outer lateral side in HPC of petunia roots.

PaPDR1 was shown to be expressed in hypodermal passage cells (HPCs), the entry point for mycorrhizal fungi [9, 24]. We therefore analyzed the sub-cellular localization of GFP-PDR1 in petunia HPCs. Root cells above the root tip of petunia are strongly auto-fluorescent (Figure 3A). However, a stronger-than-background GFP signal was visible in the outer lateral side of a few *bona fide* HPCs of np-PDR1 roots (Figure 3B, C). To identify the signal origin we reduced the auto-fluorescence background by tissue fixation for immuno-localization. GFP immuno-localization on root slices from np-PDR1 (Figure 3D-F) plants clearly showed the presence and asymmetrical localization of GFP-PDR1 at the distal-lateral plasma membrane of HPCs. Additional analyses of root segments above the root tip, where HPCs are present (Figure 3K-M) showed that *pPDR1* is also active in cortex cell layers around the

stele but not in the stele itself (Figure 3N-V). This localization suggests that SL might be cortically transported along the stele in the root and/or from the cortex towards the hypodermis to be later exuded into the rhizosphere.

Regulation of GFP-PDR1 targeting to the plasma membrane of root tip and HPCs

In order to learn more about the mechanisms involved in the cell-type specific polar distribution of PaPDR1, we performed experiments aimed at modifying the apical and outer lateral localization of PaPDR1 via auxin, GR24, or Brefeldin-A (BFA). Treatment with 25 µM BFA, which has been reported to alter vesicle trafficking responsible for targeting e.g. the auxin carriers PINs [25] and the auxinic precursor transporters ABCG36 and ABCG37 to the plasma membrane [26, 27], resulted in accumulation of small vesicles (Figure 3G-H) in 20% of the analyzed HPCs, but not in the root tip. We assumed that 2-month-old petunia roots grown on clay have a low permeability to exogenously applied compounds, possibly because of enhanced synthesis of osmoprotectans (Kosma et al., 2009).Therefore we applied 50 µM BFA combined with mild vacuum infiltrations for 90 minutes. Under this condition, we observed the accumulation of GFP-PDR1 vesicles in the analyzed HPCs and in the root tip hypodermal cells (Figure 3I, J). Auxin and GR24 treatments slightly boosted the GFP-PDR1 signal intensity 24 hours after induction, in accordance with the auxin- and strigolactone-dependent increase of *PaPDR1* expression previously observed [9] (Figure S4J-Q).

Arabidopsis PDR1-OE root tips responded to these treatments just as petunia. The asymmetric localization of GFP-PDR1 was not altered by a mock incubation; exposure to BFA caused the accumulation of vesicles in root cortex cells (Figure S4A-D), similarly to what we obtained for PhPIN2 (Figure S4E). A Sixteen-hour-long incubation with 10 µM GR24 did not alter GFP-PDR1 polar localization (Figure S4F, G), while auxin treatments strongly increased the GFP-PDR1 signal in all parts of the plasma membrane (Figure S4H, I).

Quantification of GFP-PDR1 signal after BFA treatment revealed an approximately 50% reduction in the plasma membrane in both epidermis and cortex cells (Figure S4R-V).

Petunia *pdr1* roots have reduced strigolactone transport.

We hypothesized that the observed polar localization of PaPDR1 could serve to deliver strigolactone to the shoot and HPCs, as well as to avoid accumulation of strigolactone in the biosynthetic tissues. Therefore we investigated the expression of *CCD8/DAD1*, by producing plants transgenic for a nuclear targeted YFP under the control of a 1.7 Kb-long *DAD1* promoter (*pDAD1*) [28]. Two weeks old *pDAD1:nls-YFP* seedlings showed YFP-positive nuclei only in root tips (Figure 1P, Q) . *pDAD1:nls-YFP* localization strongly overlapped with PaPDR1 and was present in root cortex cells and absent in epidermal, endodermal and stele cells of the root tip (Figure 1R). To test if the apical localized PaPDR1 contributes to strigolactone transport out of the strigolactone-synthesizing root tip, we evaluated strigolactone transport of phosphate starved *pdr1* mutants and WT (W115 x W138) using radiolabelled GR24 (Figure 4A, B). Root tips of *pdr1* mutants accumulated significantly more GR24 compared with WT. In contrast, radioactivity in agar surrounding the plantlets, in upper root segments and in shoots was higher in WT than in *pdr1* seedlings. A similar trend could be observed also in plants under sufficient P: compared with WT, *pdr1* mutant accumulated 1.7 folds higher [3H]GR24 in the root tip and transported 50% less [3H]GR24 to the shoot (n=60) . These results are compatible with a PaPDR1-dependent directional shootward transport of strigolactone.

Effects of exogenous GR24 on the main root of WT and *pdr1* petunia mutants.

To obtain further evidence whether strigolactones ectopically accumulate in the root tip in the absence of PaPDR1, we tested if WT and *pdr1* root tips were responding differently to GR24 treatment. Concentrations as low as 2.5 μM were reported to increase the number of cells in the meristematic zone in Arabidopsis root tips [6]. Two weeks old *pdr1* seedlings and the corresponding WT were germinated in the presence or absence of 2.5 μM GR24. Roots were

stained with propidium iodide, and the cells between quiescent center (QC) and the border with the elongation zone quantified (Figure S5A-F). The number of cells in the root division zone of *pdr1* mutants, but not of WT plants, was significantly increased by GR24 (Figure 4C). In contrast, the length of wild-type and *pdr1* primary roots was not significantly affected (p-value for WT +/- GR24 = 0.0569; p-value for *pdr1* +/- GR24 = 0.44140) (Figure 4C). The primary root length in *pdr1*, independent of the treatment, was shorter than in WT. So, WT and *pdr1* mutants, without GR24 treatment, have different primary root lengths but equal cell numbers in the root division zone. We then assessed if WT and *pdr1* mutants differently react to higher GR24 concentrations: we chose 10 μM GR24, which does not cause primary root length differences (Fig S1). The WT primary root cell number between quiescent center and transition zone significantly decreased by 17% ($p = 0.040$), and a stronger 37% reduction was observed for *pdr1* mutants ($p = 0.00008$) compared with mock-treated *pdr1* plants (Figure 4D and Figure S5G-J). We propose that the higher sensitivity of *pdr1* mutants to 10 μM GR24 is caused by impaired strigolactone export from the root tip. To summarize, 2.5 μM GR24 has a positive effect on *pdr1* cell divisions in root tips, as it was shown in Arabidopsis [6]. The higher 10 μM GR24 has a stronger negative effect only in *pdr1* root tip than in WT (Figure 4D). Interestingly, the changes in meristem cells abundance we observed at 2.5 μM GR24 and 10 μM GR24 do not have a significant effect on the primary root length, which is affected only by concentrations above 10 μM GR24 (Fig S1).

WT and *pdr1* mutants show different primary root lengths but have equal cell amounts in their root division zones (Figure 4C). We hypothesized that *DAD1/CCD8* expression levels might be feedback downregulated in *pdr1* mutants by the accumulation of strigolactone thus to maintain the root homeostasis. *DAD1* expression levels were indeed reduced in *pdr1* mutants at 7 and 10 days after germination (Figure 4E). Additionally, short treatments with exogenous GR24 decreased *DAD1* expression in WT petunia root tip (Figure 4F), analogous to what was shown for *MAX4* in Arabidopsis [29, 30], but not in *pdr1* mutants. Consequently, we suggest that *DAD1* downregulation in *pdr1* mutants results from strigolactone

accumulation due to an impaired strigolactone export from in *pdr1* root tips. The strigolactone altered biosynthetic levels might be then responsible for the differential growth of the primary root in WT and *pdr1* mutants possibly via crosstalk with auxin [22, 29].

Discussion

Our results indicate that the specific localization of the strigolactone transporter PaPDR1 allows to fulfill a number of different tasks in petunia roots. PaPDR1 exports strigolactones from the root tip shootwards, either for further exudation to soil or regulation of lateral shoot branching. In addition, our results indicate that the export of strigolactones from their site of biosynthesis is required to ensure continuous production of these phytohormones.

A question still to be addressed is if and how root- and shoot-derived strigolactones interact and how this is modulated by transport processes. At the moment it is difficult to quantify the likelihood of such transport regulation in other plant species than petunia. The recent isolation of NtPDR6 (Xie et al., 2014), an ABCG transporter possibly involved in strigolactone transport in tobacco, raises the possibility that in the Solanaceae strigolactone transport is regulated in a similar way. The stimulation of lateral bud outgrowth through reduced SL levels occurs either by direct downregulation of transcription factors like BRC1 [31, 32] necessary for bud outgrowth or by stimulating auxin export from dormant buds by increasing PIN1 abundance [22, 29]. Interestingly PIN1 inhibition was observed in petunia PDR1-OE root tips without the need for GR24 treatment, indicating that a similar cross-talk takes place above- as well below-ground. Further analyses need to be conducted in tissues where strigolactones and auxins, or other hormones, have been shown to have overlapping domains, e.g. where secondary growth [7], adventitious root formation [5] and internode elongation [33] occur. Unfortunately, the root tip is the sole tissue in petunia exhibiting

limited autofluorescence allowing to get conclusive localization results, therefore we could not further elucidate this process in other, more distal root segments or the shoot. Nevertheless, based on GFP-PDR1 apical localization in the root tip and on the nuclear localized pPDR1:YFP expression pattern we observed, we hypothesize that SL transport occurs not or not only via the vasculature as was previously reported [16] but also via cortex cells surrounding the stele. This hypothesis is supported by the fact that after feeding roots with radiolabelled GR24, fewer radioactivity is observed in the shoot of the strigolactone transporter mutant.

We show here that PaPDR1, similarly to PIN2 [21], can target different membrane domains in distinct cell populations. However, to our knowledge this is the first time a transmembrane protein is detected either in the apical/basal or in the lateral domain of different cell types. No transcriptome of HPCs is available yet and it is therefore premature to speculate which mechanisms are responsible for PaPDR1 localization in these specific cells. In the petunia root hypodermis, PaPDR1 is apical localized. Interestingly, in GR24 treated PDR1-OE petunia seedlings, PaPDR1 is additionally co-expressed with a strongly down-regulated PhPIN1 in the root stele. These results suggest that PaPDR1 might share some players of the vesicle targeting system also involved in the localization of PINs or other trans-membrane proteins [34, 35]. For PIN proteins, the amino acid motif TPRXS(N/S) situated in the large central hydrophilic loop is crucial for phosphorylation and polar localization but this motif is absent in PaPDR1. Putative phosphorylation sites in PaPDR1 are currently under investigation to assess their involvement in PaPDR1 localization.

Polar phytohormone transport was until now reported exclusively for auxins [36]. Cytokinins, jasmonate and its metabolite methyl-jasmonate are transported either via xylem or phloem for long-distance signaling [37, 38]. The characterization of a cytokinin transporter is limited to low-affinity systems for both cytokinins and adenine [39] and to ABCG14 [40, 41], the latter essential for root to shoot translocation of cytokinin, but not described as polarly localized. Also the recently reported shoot to root transport of cytokinins to regulate nodulation in

legumes is likely to happen via the vasculature [42]. Transporters for abscisic acid (ABA) were recently identified in Arabidopsis as the ABCG class protein ABCG25 [43] and ABCG40 [44] and the low-affinity nitrate transporter NPF4.6/NRT1.2 [45, 46]. They both regulate cellular uptake of ABA but no asymmetrical localization on the plasma membrane is known. Brassinosteroids are not reported for long-distance transport [47] and gibberellins are suggested to be transported symplastically through diffusion [48]. The GR24-induced ectopic PaPDR1 pattern suggests that strigolactone might play a role not only in enhancing *PaPDR1* expression but also in increasing PaPDR1 stability. The observation that GR24 induces or stabilizes PaPDR1 possibly promoting its own polar transport in cells where it is present might be a further commonality with auxin [49]. Also auxin seems to play a role in shaping *PaPDR1* expression and its localization. The downregulation of PIN1 in petunia PDR1-OE root tips is compatible with pPDR1 being a mediator of the auxin-strigolactone network (Figure S2V) [22]. Interestingly, AtPIN1 is not downregulated in PDR1-OE Arabidopsis. This fits with the disagreement whether in Arabidopsis exogenous GR24 triggers the downregulation of PIN1 in root tips [6, 22]. Furthermore, in Arabidopsis endogenous strigolactone levels are lower compared to other Solanaceae like tomato [16, 50] and hence even increasing strigolactone transport might not interfere with PIN localization.

Additional post-transcriptional/post-translational modifications may play an important role in PaPDR1 regulation. Despite the 35S promoter, PDR1-OE petunia plants still show a preferential PaPDR1 protein abundance into the root tip hypodermis and HPCs, in contrast to the broader *pPDR1:nls-YFP* pattern. Also, protein quantification in np-PDR1 petunias at different developmental stages (Figure 1 and Figure S2M, N) supports the hypothesis that PaPDR1 protein degradation might be a way to regulate strigolactone transport.

Amounts of exogenous SL as low as 2.5 μM were reported to alter cell division in root meristems of WT Arabidopsis seedlings [6]. We show here that *pdr1* mutants are also sensitive to SL concentrations as low as 2.5 μM, which do not have effects on WT petunia primary root length or meristematic cell numbers. These results show that petunia, as long as

PaPDR1 is functional, is less sensitive to GR24 than Arabidopsis, possibly because of petunia higher capability of exudating SL as attractant to mycorrhizal fungi. On the contrary, 10 μM GR24 negatively affect the meristematic cell number both in WT and *pdr1* seedlings, but still more dramatically in *pdr1* mutants, in line with their impaired SL transport. Primary root lengths of WT and *pdr1* mutants are not as affected by either 2.5 or 10 μM GR24 as meristematic cell number. Additional studies are necessary to investigate not only the effects on cell division of endogenous and exogenous SL changes, but also on cells leaving the root meristem. The effects of SL accumulation in petunia root tips on auxin and cytokinin, known players in patterning the root meristem [51], are still to be studied. Lateral root density in petunia is only transiently affected by GR24 in contrast to primary root length. Investigations are ongoing in our lab to understand if cells close to lateral root primordia, reported in rice to be among the tissues preferentially colonized by fungi [52] are also enriched for *PDR1* expression and/or HPC presence, can also exude the applied GR24 more easily than other root parts and thus partially suppress GR24-induced lateral root inhibition.

Strigolactone transport from biosynthetic to target tissues is therefore highly regulated by endogenous and exogenous signals and crosstalk between strigolactone and auxin biosynthesis. Such complex hormonal network and gene expression synchronization in root cells is not only necessary to ensure that SL does not alter the root meristem homeostasis, but also to modulate the amount of strigolactone transported shootward. PaPDR1 seems to play an important role in integrating and synchronizing feedback signals generated by nutrient availability, strigolactone and auxin distribution.

Acknowledgements

We thank Dr. José María Mateos (University of Zurich, Switzerland) for providing us with the vibratome. Prof. Dolf Weijers (Wageningen University, the Netherlands) for shipping us his set of Ligation-Independent-Cloning vectors. Prof. Bruno Humbel (University of Lausanne, Switzerland) for suggestions on GFP-PDR1 detection. Dr. Undine Krügel (University of

Zurich, Switzerland) and Prof. Michal Jasinski (Polish Academy of Science, Poland) for hints on protein quantification.

Figure legends

Figure 1. Localization of PDR1 and DAD1 via protein quantification and CLSM analysis

(A-C) GFP-PDR1 quantification in 10-day-old petunia seedlings: (A) WT, (B) *pPDR1:GFP-PDR1* (np-PDR1), (C) *p35S:GFP-PDR1* (PDR1-OE). (D-E) GFP-PDR1 quantification in 10-day-old Arabidopsis *rdr6* seedlings: (D) *pPDR1:GFP-PDR1* and (E) *p35S:GFP-PDR1* (At PDR1-OE). (A' to E') Comassie blue controls relative to (A-E). (F-I) GFP-PDR1 in petunia root tip hypodermal cells of: (F, arrowhead) 2-month-old np-PDR1 plants starved on clay, (G, arrowhead) 2-week-old PDR1-OE seedlings. (H) 4-week-old np-PDR1 plants after phosphate starvation and (I, arrowhead) light and GFP channels merged. (J-L) Propidium iodide staining of petunia root-tip cell walls: (J) epidermis. (K) hypodermis and (L) stele. (M-O) Anti-GFP immuno-localization on PDR1-OE seedlings: (M) epidermis, (N) hypodermis and (O) cortex. (P-R) *pDAD1:nls-YFP* expression in roots of 2 weeks old petunia: (P) longitudinal view of the root tip, (Q) cross section of a differentiated root, (R) cross section of the root tip: *pDAD1* is active in hypodermal and cortex layers between epidermis and endodermis and absent in the stele. * = 150 KDa; scale bars = 20 μm. See also Figure S1

Figure 2. GFP-PDR1 sub-cellular localization via CLSM analysis.

(A-F) Immuno-localization on PhPIN2 (green) and GFP-PDR1 (red) in PDR1-OE root tips: PhPIN2 is present in (A) hypodermis and (D) cortex, GFP-PDR1 only in hypodermis (B) and not in cortex (E). (G-I) Co-localization of PhPIN2 and GFP-PDR1. (J-K) Immuno-localization on PhPIN2 (red) and GFP-PDR1 (green) on starved np-PDR1. (L) light channel, (M) merge of J, K and L. (N-P) Immuno-localization on AtPIN2 (red) and GFP-PDR1 (green) in PDR1-OE At seedlings, cortex. (Q-S) Immuno-localization on AtPIN1 (red) and GFP-PDR1 (green) in PDR1-OE At seedlings, stele. (T-V) PhPIN2 (green) and GFP-PDR1 (red) n the cortex of

PDR1-OE after incubation with 10 μM GR24. (W-Y) PhPIN1 (green) and GFP-PDR1 (red) in the stele of PDR1-OE seedlings after incubation with 10 μM GR24. (Z, Z') Digital quantification (ImageJ) of PDR1 and PhPIN2 signals, either cytosolic or plasma-membrane localized. The significances of differences between PDR1 and PhPIN2 signals were calculated via Student's T-test. For cytosolic measurements: PDR1-OE ($p < 0.0005$), PDR1-OE GR24 ($p < 0.0005$). For plasma membrane measurements: npPDR1 ($p < 0.0005$), PDR1-OE GR24 ($p < 0.005$).

Scale bars = 20 μm. See also Figure S2

Figure 3. GFP-PDR1 localization in HPC and differentiated roots and sensitivity to BFA via CLSM analysis.

(A) Petunia root autofluorescence (B-C) GFP-PDR1 in np-PDR1 radial root sections: arrowheads indicate GFP-PDR1 in HPCs. (D) autofluorescence (red channel) (E-F) GFP immuno-localization on np-PDR1 roots, transversal sections. (G) GFP-PDR1 in HPC of np-PDR1 plants, longitudinal view. (H) Vesicles accumulate in HPC after BFA incubation. (I) GFP-PDR1 in hypodermal cells of petunia root tip. (J) Vesicles accumulate in hypodermal cells after BFA incubation. (K) Nuclear localized pPDR1:YFP in HPC (arrowhead), (L) root autofluorescence (red channel) and merging (M). (N) pPDR1:YFP cortical localized, (O) plastidial red autofluorescence and merging (P). (Q) pPDR1:YFP is absent in the stele, which is surrounded by red autofluorescent plastids (R) and merging (S). (T-V) Radials section of the root segment showed in (Q-S): pPDR1:YFP is present in HPC (T, arrowhead) but not in the stele. Scale bars A-J = 20 μm; K-V = 50 μM. See also Figure S3 and S4.

Figure 4. Effects of strigolactone accumulation in root tips.

(A) Scheme for the transport quantification of [3H]GR24 in root tips, root segments (middle and top), shoots and agar samples (n=11). (B) Quantification of [3H]GR24 transport in 2 weeks old WT and *pdr1* plants: *pdr1* root tips accumulate 4-folds higher SL than WT, exude

to agar 0.5-fold SL less than WT and transport less [3H]GR24 shootward. (C) Lengths of primary roots (dark grey bars) (n=40) and cell number (light grey bars) in root division zones of 2-week-old WT and *pdr1* mutants (n=18). Growth on 2.5 μM GR24 increases the cell number in root division zones of *pdr1* mutants but not of WT (n=8). (D) Growth on 10 μM GR24 decreases the cell number in root division zones of *pdr1* (minus 37% p = 0.00008) and WT (minus 17%, p = 0.040) (n=8). (E) *DAD1* expression relative to GAPDH in petunia root tips. *DAD1* is 6-folds downregulated in *pdr1* root tips compared to WT at 7 and 10 days after germination (p = 0.030 and 0.016). (F) After 6 hours incubation in 1 μM GR24, *DAD1* expression level is 30% decreased in WT seedlings (p = 0.035). (* = P < 0.05; ** = P < 0.005; ** = P < 0.0005 from Student's T-test). Data are represented as mean ± SEM. See also Figure S5.

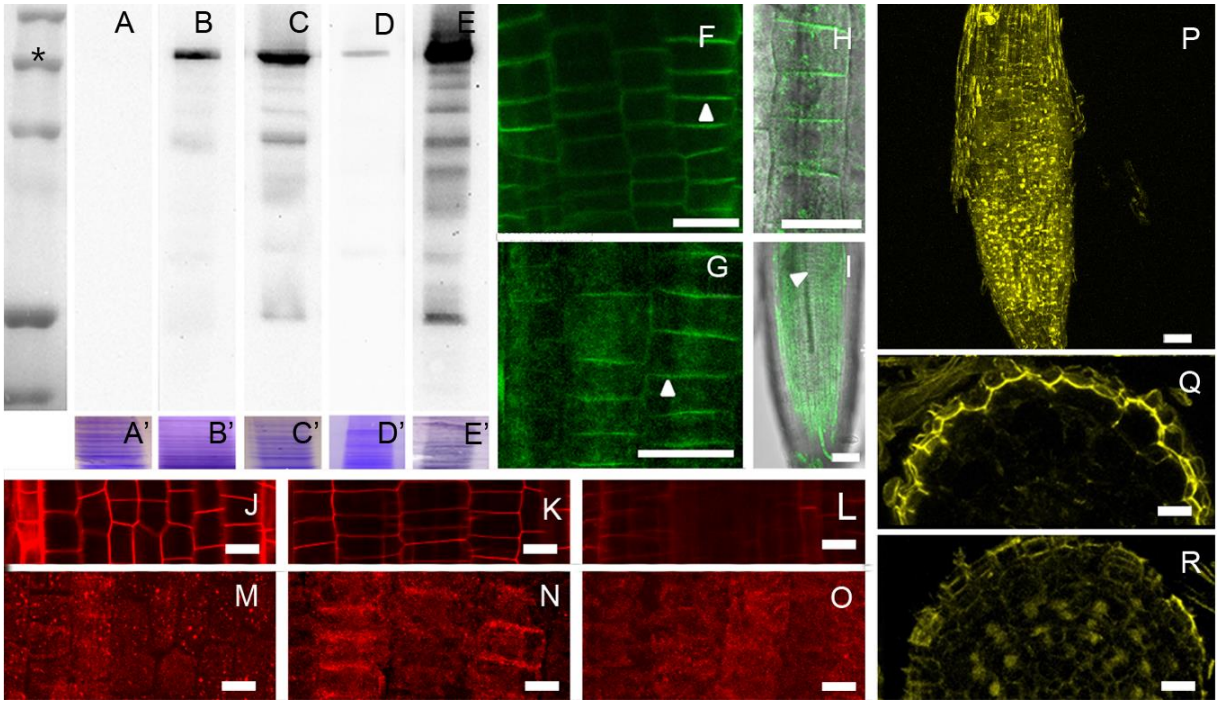

Figure 1

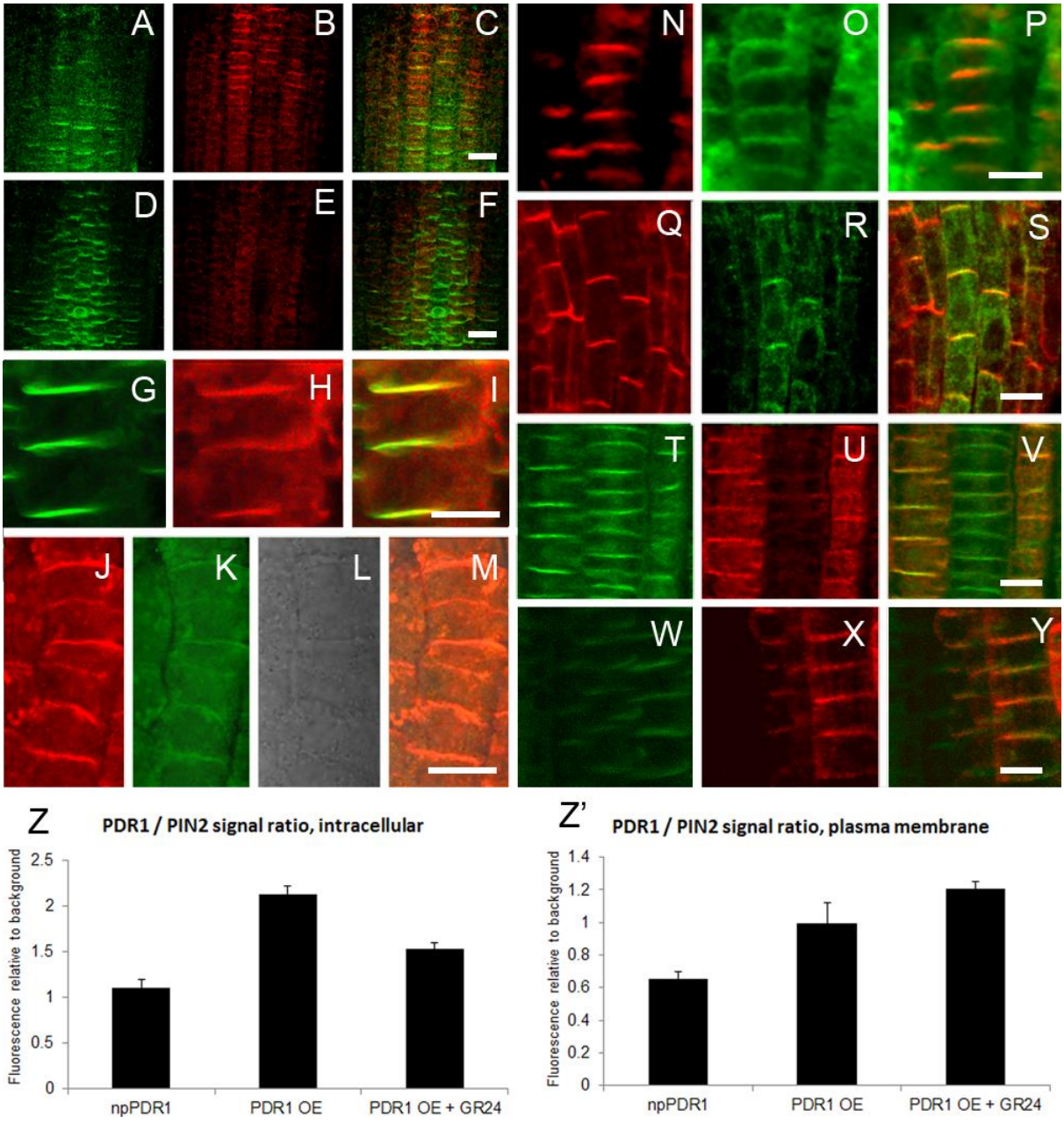
A
B
C
D
E
F
G
H
I
J
K
L
M
N
O
P
Q
R
S
T
U
V
W
X
Y
Z
PDR1 / PIN2 signal ratio, intracellular
Fluorescence relative to background
2.5
2
1.5
1
0.5
0
npPDR1
PDR1 OE
PDR1 OE + GR24
Z'
PDR1 / PIN2 signal ratio, plasma membrane
Fluorescence relative to background
1.4
1.2
1
0.8
0.6
0.4
0.2
0
npPDR1
PDR1 OE
PDR1 OE + GR24

Figure 2

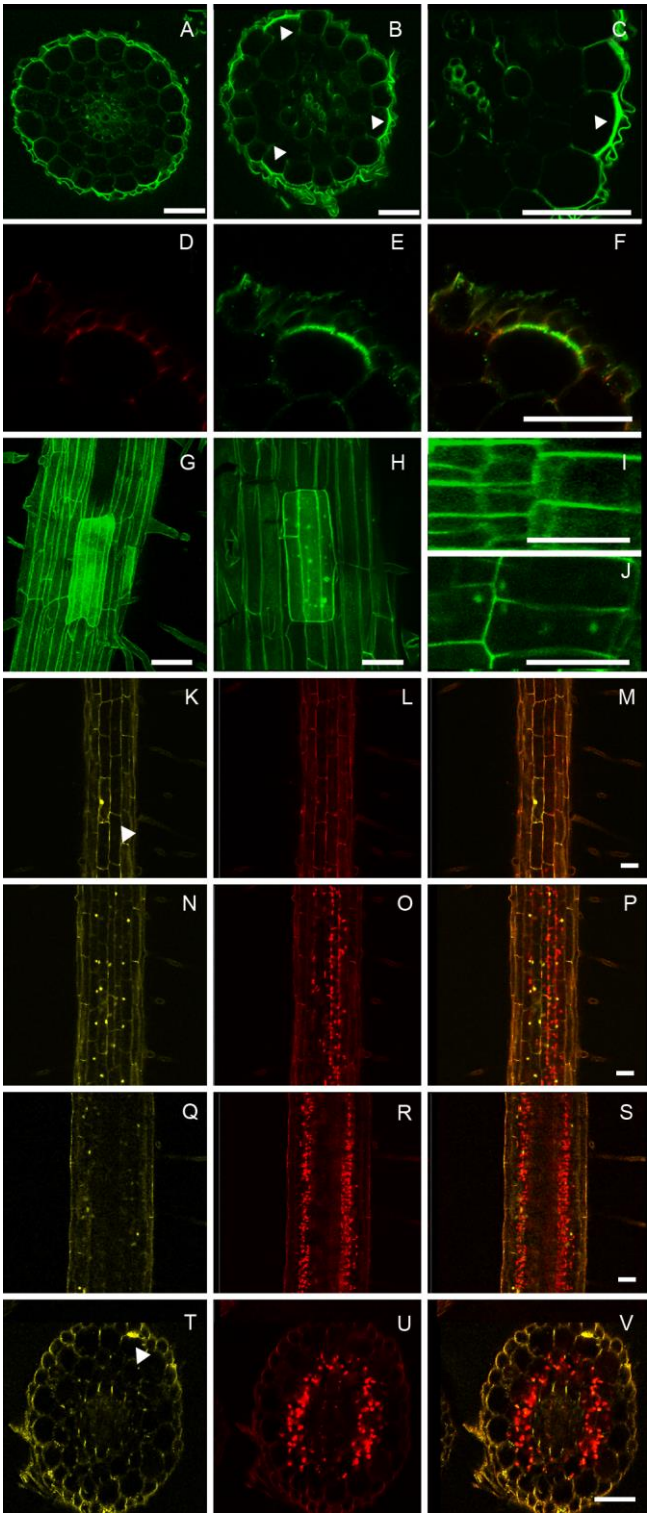

Figure 3

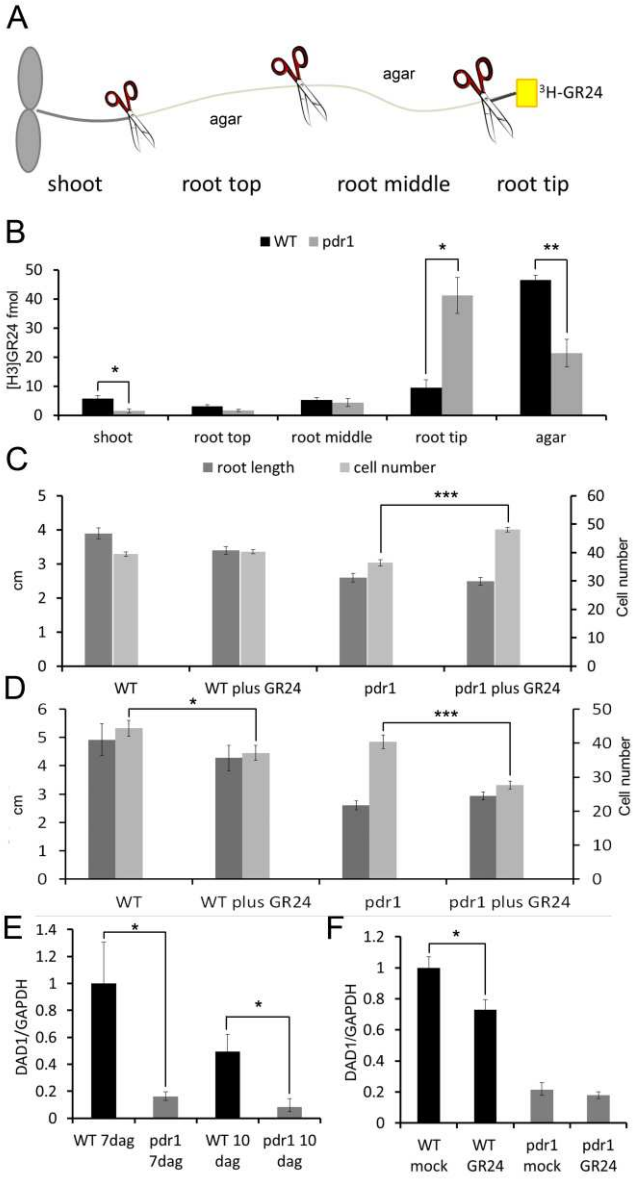
A
agar
agar
^{3}H-GR24
shoot
root top
root middle
root tip
B
WT
pdr1
[H3]GR24 fmol
shoot
root top
root middle
root tip
agar
C
root length
cell number
cm
Cell number
WT
WT plus GR24
pdr1
pdr1 plus GR24
D
cm
Cell number
WT
WT plus GR24
pdr1
pdr1 plus GR24
E
DAD1/GAPDH
WT 7dag
pdr1 7dag
WT 10 dag
pdr1 10 dag
F
DAD1/GAPDH
WT mock
WT GR24
pdr1 mock
pdr1 GR24

Figure 4

Literature

1. Cook, C.E., Whichard, L.P., Turner, B., Wall, M.E., and Egley, G.H. (1966). Germination of Witchweed (Striga lutea Lour.): Isolation and Properties of a Potent Stimulant. Science *154*, 1189-1190.
2. Akiyama, K., Matsuzaki, K., and Hayashi, H. (2005). Plant sesquiterpenes induce hyphal branching in arbuscular mycorrhizal fungi. Nature *435*, 824-827.
3. Gomez-Roldan, V., Fermas, S., Brewer, P.B., Puech-Pages, V., Dun, E.A., Pillot, J.P., Letisse, F., Matusova, R., Danoun, S., Portais, J.C., et al. (2008). Strigolactone inhibition of shoot branching. Nature *455*, 189-194.
4. Umehara, M., Hanada, A., Yoshida, S., Akiyama, K., Arite, T., Takeda-Kamiya, N., Magome, H., Kamiya, Y., Shirasu, K., Yoneyama, K., et al. (2008). Inhibition of shoot branching by new terpenoid plant hormones. Nature *455*, 195-200.
5. Rasmussen, A., Mason, M.G., De Cuyper, C., Brewer, P.B., Herold, S., Agusti, J., Geelen, D., Greb, T., Goormachtig, S., Beeckman, T., et al. (2012). Strigol actones Suppress Adventitious Rooting in Arabidopsis and Pea. Plant Physiology *158*, 1976-1987.
6. Ruyter-Spira, C., Kohlen, W., Charnikhova, T., van Zeijl, A., van Bezouwen, L., de Ruijter, N., Cardoso, C., Lopez-Raez, J.A., Matusova, R., Bours, R., et al. (2011). Physiological effects of the synthetic strigolactone analog GR24 on root system architecture in Arabidopsis: another belowground role for strigolactones? Plant Physiol *155*, 721-734.
7. Agusti, J., Herold, S., Schwarz, M., Sanchez, P., Ljung, K., Dun, E.A., Brewer, P.B., Beveridge, C.A., Sieberer, T., Sehr, E.M., et al. (2011). Strigolactone signaling is required for auxin-dependent stimulation of secondary growth in plants. Proc Natl Acad Sci U S A *108*, 20242-20247.
8. Snowden, K.C., Simkin, A.J., Janssen, B.J., Templeton, K.R., Loucas, H.M., Simons, J.L., Karunairetnam, S., Gleave, A.P., Clark, D.G., and Klee, H.J. (2005). The Decreased apical dominance 1/petunia hybrida carotenoid cleavage dioxygenase8 gene affects branch production and plays a role in leaf senescence, root growth, and flower development. Plant Cell *17*, 746-759.
9. Kretzschmar, T., Kohlen, W., Sasse, J., Borghi, L., Schlegel, M., Bachelier, J.B., Reinhardt, D., Bours, R., Bouwmeester, H.J., and Martinoia, E. (2012). A petunia ABC protein controls strigolactone-dependent symbiotic signalling and branching. Nature *483*, 341-U135.
10. Wang, Y., and Li, J. (2011). Branching in rice. Curr Opin Plant Biol *14*, 94-99.

11. Xie, X., and Yoneyama, K. (2010). The strigolactone story. Annu Rev Ph ytopathol *48*, 93-117.
12. Alder, A., Jamil, M., Marzorati, M., Bruno, M., Vermathen, M., Bigler, P., Ghisla, S., Bouwmeester, H., Beyer, P., and Al-Babili, S. (2012). The Path from beta-Carotene to Carlactone, a Strigolactone-Like Plant Hormone. Science *335*, 1348-1351.
13. Ruyter-Spira, C., Al-Babili, S., van der Krol, S., and Bouwmeester, H. (2013). The biology of strigolactones. Trends Plant Sci *18*, 72-83.
14. Bainbridge, K., Sorefan, K., Ward, S., and Leyser, O. (2005). Hormonally controlled expression of the Arabidopsis MAX4 shoot branching regulatory gene. Plant J *44*, 569-580.
15. Sorefan, K., Booker, J., Haurogne, K., Goussot, M., Bainbridge, K., Foo, E., Chatfield, S., Ward, S., Beveridge, C., Rameau, C., et al. (2003). MAX4 and RMS1 are orthologous dioxygenase-like genes that regulate shoot branching in Arabidopsis and pea. Gene Dev *17*, 1469-1474.
16. Kohlen, W., Charnikhova, T., Liu, Q., Bours, R., Domagalska, M.A., Beguerie, S., Verstappen, F., Leyser, O., Bouwmeester, H., and Ruyter-Spira, C. (20 11). Strigolactones are transported through the xylem and play a key role in shoot architectural response to phosphate deficiency in nonarbuscular mycorrhizal host Arabidopsis. Plant Physiol *155*, 974-987.
17. Butaye, K.M., Goderis, I.J., Wouters, P.F., Pues, J.M., Delaure, S.L., Broekaert, W.F., Depicker, A., Cammue, B.P., and De Bolle, M.F. (2004). Stable high -level transgene expression in Arabidopsis thaliana using gene silencing mutants and matrix attachment regions. Plant J *39*, 440-449.
18. Wegmuller, S., Svistoonoff, S., Reinhardt, D., Stuurman, J., Amrhein, N., and Bucher, M. (2008). A transgenic dTph1 insertional mutagenesis system for forward genetics in mycorrhizal phosphate transport of Petunia. Plant J *54*, 1115-1127.
19. Ha, C.V., Leyva-Gonzalez, M.A., Osakabe, Y., Tran, U.T., Nishiyama, R., Watanabe, Y., Tanaka, M., Seki, M., Yamaguchi, S., Dong, N.V., et al. (2014). Positive regulatory role of strigolactone in plant responses to drought and salt stress. Proc Natl Acad Sci U S A *111*, 851-856.
20. Yang, S.Y., and Paszkowski, U. (2011). Phosphate import at the arbuscule: just a nutrient? Mol Plant Microbe Interact *24*, 1296-1299.
21. Krecek, P., Skupa, P., Libus, J., Naramoto, S., Tejos, R., Friml, J., and Zazimalova, E. (2009). The PIN -FORMED (PIN) protein family of auxin transporters. Genome Biol *10*.

22. Shinohara, N., Taylor, C., and Leyser, O. (2013). Strigolactone can promote or inhibit shoot branching by triggering rapid depletion of the auxin efflux protein PIN1 from the plasma membrane. PLoS Biol *11*, e1001474.
23. Pandya-Kumar, N., Shema, R., Kumar, M., Mayzlish-Gati, E., Levy, D., Zemach, H., Belausov, E., Wininger, S., Abu-Abied, M., Kapulnik, Y., et al. (2014). Strigolactone analog GR24 triggers changes in PIN2 polarity, vesicle trafficking and actin filament architecture. New Phytol *202*, 1184-1196.
24. Sharda, J.N., and Koide, R.T. (2008). Can hypodermal passage cell distribution limit root penetration by mycorrhizal fungi? New Phytol *180*, 696-701.
25. Geldner, N., Friml, J., Stierhof, Y.D., Jurgens, G., and Palme, K. (2001). Auxin transport inhibitors block PIN1 cycling and vesicle traficking. Nature *413*, 425-428.
26. Ruzicka, K., Strader, L.C., Bailly, A., Yang, H.B., Blakeslee, J., Langowski, L., Nejedla, E., Fujita, H., Itoh, H., Syono, K., et al. (2010). Arabidopsis PIS1 encodes the ABCG37 transporter of auxinic compounds including the auxin precursor indole-3-butyric acid. P Natl Acad Sci USA *107*, 10749-10753.
27. Strader, L.C., and Bartel, B. (2009). The Arabidopsis PLEIOTROPIC DRUG RESISTANCE8/ABCG36 ATP Binding Cassette Transporter Modulates Sensitivity to the Auxin Precursor Indole-3-Butyric Acid. Plant Cell *21*, 1992-2007.
28. De Rybel, B., van den Berg, W., Lokerse, A., Liao, C.Y., van Mourik, H., Moller, B., Peris, C.L., and Weijers, D. (2011). A versatile set of ligation -independent cloning vectors for functional studies in plants. Plant Physiol *156*, 1292-1299.
29. Hayward, A., Stirnberg, P., Beveridge, C., and Leyser, O. (2009). Interac tions between auxin and strigolactone in shoot branching control. Plant Physiol *151*, 400-412.
30. Liang, J., Zhao, L., Challis, R., and Leyser, O. (2010). Strigolactone regulation of shoot branching in chrysanthemum (Dendranthema grandiflorum). J Exp Bot *61*, 3069-3078.
31. Gonzalez-Grandio, E., Poza-Carrion, C., Sorzano, C.O., and Cubas, P. (2013). BRANCHED1 promotes axillary bud dormancy in response to shade in Arabidopsis. Plant Cell *25*, 834-850.
32. Gonzalez-Grandio, E., and Cubas, P. (2014). Identifica tion of gene functions associated to active and dormant buds in Arabidopsis. Plant Signal Behav *9*, e27994.
33. de Saint Germain, A., Ligerot, Y., Dun, E.A., Pillot, J.P., Ross, J.J., Beveridge, C.A., and Rameau, C. (2013). Strigolactones stimulate internod e elongation independently of gibberellins. Plant Physiol *163*, 1012-1025.

34. Korbei, B., and Luschnig, C. (2013). Plasma membrane protein ubiquitylation and degradation as determinants of positional growth in plants. J Integr Plant Biol *55*, 809-823.
35. Offringa, R., and Huang, F. (2013). Phosphorylation -dependent Trafficking of Plasma Membrane Proteins in Animal and Plant Cells. J Integr Plant Biol *55*, 789-808.
36. Petrasek, J., and Friml, J. (2009). Auxin transport routes in plant development. Development *136*, 2675-2688.
37. Sakakibara, H. (2006). Cytokinins: activity, biosynthesis, and translocation. Annu Rev Plant Biol *57*, 431-449.
38. Thorpe, M.R., Ferrieri, A.P., Herth, M.M., and Ferrieri, R.A. (2007). 11C -imaging: methyl jasmonate moves in both phloem and xylem, promotes transport of jasmonate, and of photoassimilate even after proton transport is decoupled. Planta *226*, 541-551.
39. Cedzich, A., Stransky, H., Schulz, B., and Frommer, W.B. (2008). Characterization of cytokinin and adenine transport in Arabidopsis cell cultures. Plant Physiol *148*, 1857-1867.
40. Ko, D., Kang, J., Kiba, T., Park, J., Kojima, M., Do, J., Kim, K.Y., Kwon, M., Endler, A., Song, W.Y., et al. (2014). Arabidopsis ABCG14 is essential for the root -to-shoot translocation of cytokinin. Proc Natl Acad Sci U S A *111*, 7150-7155.
41. Zhang, K., Novak, O., Wei, Z., Gou, M., Zhang, X., Yu, Y., Yang, H., Cai, Y., Strnad, M., and Liu, C.J. (2014). Arabidopsis ABCG14 protein controls the acropetal translocation of root-synthesized cytokinins. Nat Commun *5*, 3274.
42. Sasaki, T., Suzaki, T., Soyano, T., Kojima, M., Sakakibara, H., and Kawaguchi, M. (2014). Shoot -derived cytokinins systemically regulate root nodulation. Nat Commun *5*, 4983.
43. Kuromori, T., Miyaji, T., Yabuuchi, H., Shimizu, H., Sugimoto, E., Kamiya, A., Moriyama, Y., and Shinozaki, K. (2010). ABC transporter AtABCG25 is involved in abscisic acid transport and responses. Proc Natl Acad Sci U S A *107*, 2361-2366.
44. Kang, J., Hwang, J.U., Lee, M., Kim, Y.Y., Assmann, S.M., Martinoia, E., and Lee, Y. (2010). PDR -type ABC transporter mediates cellular uptake of the phytohormone abscisic acid. Proc Natl Acad Sci U S A *107*, 2355-2360.
45. Kanno, Y., Hanada, A., Chiba, Y., Ichikawa, T., Nakazawa, M., Matsui, M., Koshiba, T., Kamiya, Y., and Seo, M. (2012). Identification of an abscisic acid transporter by functional screening using the receptor complex as a sensor. Proc Natl Acad Sci U S A *109*, 9653-9658.
46. Leran, S., Varala, K., Boyer, J.C., Chiurazzi, M., Crawford, N., Daniel-Vedele, F., David, L., Dickstein, R., Fernandez, E., Forde, B., et al. (2014). A unified

nomenclature of NITRATE TRANSPORTER 1/PEPTIDE TRANSPORTER family members in plants. Trends Plant Sci *19*, 5-9.

47. Symons, G.M., Ross, J.J., Jager, C.E., and Reid, J.B. (2008). Brassinosteroid transport. J Exp Bot *59*, 17-24.
48. Bruggeman, F.J., Libbenga, K.R., and Van Duijn, B. (2001). The diffusive transport of gibberellins and abscisic acid through the aleurone layer of germinating barley grain: a mathematical model. Planta *214*, 89-96.
49. Paciorek, T., Zazimalova, E., Ruthardt, N., Petrasek, J., Stierhof, Y.D., Kleine-Vehn, J., Morris, D.A., Emans, N., Jurgens, G., Geldner, N., et al. (2005). Auxin inhibits endocytosis and promotes its own efflux from cells. Nature *435*, 1251-1256.
50. Goldwasser, Y., Yoneyama, K., Xie, X., and Yoneyama, K. (2008). Production of Strigolactones by Arabidopsis thaliana responsible for Orobanche aegyptiaca seed germination. Plant Growth Regulation *55*, 21-28.
51. Ruzicka, K., Simaskova, M., Duclercq, J., Petrasek, J., Zazimalova, E., Simon, S., Friml, J., Van Montagu, M.C., and Benkova, E. (2009). Cytokinin regulates root meristem activity via modulation of the polar auxin transport. Proc Natl Acad Sci U S A *106*, 4284-4289.
52. Gutjahr, C., and Paszkowski, U. (2013). Multiple control levels of root system remodeling in arbuscular mycorrhizal symbiosis. Front Plant Sci *4*, 204.